"FAST" CFD METHODS IN AIRCRAFT SYSTEM DESIGN. APPLICATION TO C295W MODIFICATIONS.

Carlos González Biedma
Airbus Defence & Space SAU
Carlos.Z.Gonzalez@airbus.com
Keywords: *Aerodynamics - Computational Fluid Dynamics*

Abstract

For the Airbus C295 continuous product improvement is required to fulfil new missions and thus satisfy an increased amount of customers. New capabilities demand changes in systems as well as modifications in the airframe. Shorter development times have changed the approach of the aerodynamic design with less wind tunnel campaigns before first flight. New "Fast" CFD has been introduced to reduce the development time of modifications.

The process to develop a new sponson with redesigned landing gear doors using this Fast CFD methodology is used as an example. CFD results are compared with wind tunnel and flight test data.

1 General Introduction

A new "FAST" CFD process has been developed for simpler, less costly, short time and accurate modification estimation in complete aircraft configurations. Highly automated topology extraction, mesh generation, solver and post-processing have been enabled and successfully integrated in the C295W. In this paper, the CFD process is briefly described and some results of very complex aircraft configurations are compared with wind tunnel and flight test data.

2 Topology

C295W CATIA files are used directly and exported to high resolution Virtual Reality Markup Language (WRL) files. Since in almost all cases, thousands of parts are present, grouping of parts/assemblies and renaming is necessary for easier identification of regions of interest. Matlab scripts to perform this task have been developed to sort parts by size, removal of duplicated parts, removal of small components if required, making of convex hulls for complex parts, geometric simplification, etc in an automatic way. ICEM CFD geometry files are created for easier visualization and topology checking before exporting them to STL geometric files.

A modular approach for the aircraft topology is used to build any possible configuration. Many files in the STL format are created for individual components (flap settings, control deflection, landing gear positions, open/closed ramps or doors, etc …) in order to be able to create any possible setting or even some failure modes. An assembled geometry is shown in the Fig. 1 with different color for some of the interchangeable components.

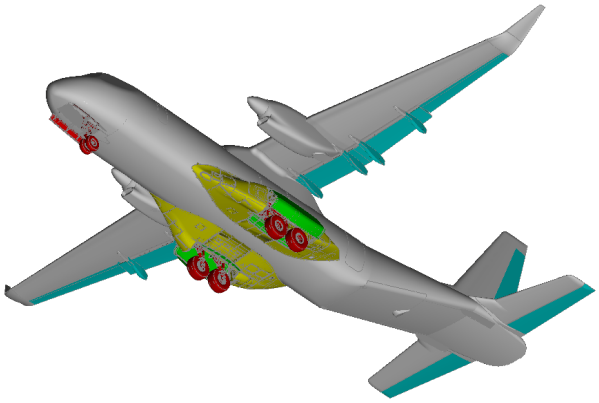

Fig. 1. Modular topology.

2.1 Deformation

For highly elastic components, such as wings, landing gear doors, etc … the CATIA

geometry is in JIG shape and needs to be transformed to 1g flight shape before starting the meshing process. For most components a simple coordinate system transformation is possible but for others is not. Landing gear doors for example are bent and twisted in 1g flight condition so the means of "flexing" the topology is required. In our case, a simple network of Radial Basis Functions (RBF) from the jig shape using Inverse Distance Weighting (IDW) is used. This methodology is only applied to the point cloud of the triangulated geometry files. Fig. 2 shows the jig shape (in grey) and the 1g flight shape (in red).

Fig. 2. Deformed topology.

3 Meshing

A Cartesian, hanging node, cut cell "modular" mesh with extruded boundary layer approach has been used in order to account for fast mesh modification turnaround time, replacing expensive (and very time consuming) structured multi-block grids.

To simulate the propeller, additional structured meshes with non-conformal interfaces are used to simulate propeller effects with a Virtual Blade Model (VBM) for time averaged RANS calculations while unstructured or cartesian cut cell meshes have been used when simulating the moving propeller on URANS computations.

3.1 Mesh Generation

For mesh generation, the open-source tool SnappyHexMesh (SHM) version 2.3 and 3.0+ from the OpenFOAM suite (see [1] and [2]) has been selected. It uses a cut-cell octree cartesian mesh approach with extruded boundary layer. This approach yields polygonal meshes with hanging nodes that not all solvers can handle. Aircraft topology is discretized as triangulated surfaces in STL ASCII format. As a modular approach is used for the geometry, large numbers of STL files are required for a mesh computation: 78 STLs for the geometry of a C295W with gear down and 15 additional STLs for the wake refinement.

To avoid large volumetric changes in the mesh near the topology, a constant size approach for the surfaces is used. That is, the same size is used for each individual surface and size changes are tried to be keep at a minimum.

A "brute force" strategy has been used for the wake generation and a very large number of cells are present in this wake. Fig. 3 shows the typical wake used for the C295 in the symmetry plane.

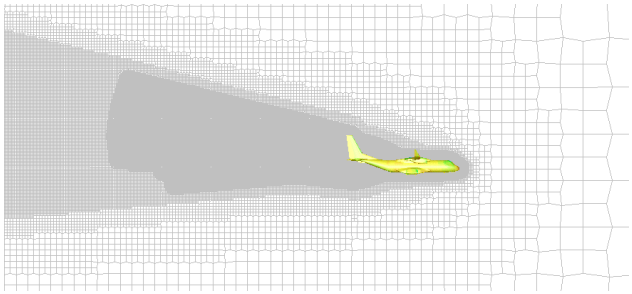

Fig. 3. Symmetry plane mesh.

A high Reynolds number wall function turbulence model is to be used in the solver, thus, a first layer thickness for y+ between 30-60 has been selected and a few additional cells extruded for solution stability. Typically 4 to 5 cells with expansion of 1.25 are used.

Transition between cell levels is also important for solver stability: meshes with transition of 2 and 4 cells between levels have been tried, yielding better results the latter but with a non-negligible increase in the cell count.

Due to the modular topology approach used, very complex aircraft configurations can be created with ease; even internal components can be added in combination with any external aero configuration.

3.2 Mesh Sizes

Average mesh size for half aircraft is around 75 million cells, although in some cases larger meshes have been used.

On these meshes, approximately 25% of the cells correspond to the surface discretization and external fluid volume, 44% to the wake and 31% to the near flow and the boundary layer. Thus, some additional work on coarser meshes by means of reducing the wake cell count would be possible.

Most of the meshing process activities are performed in parallel with 32 or 64 CPUs depending on mesh size. Typical wall times are around 2.8 hrs and 75 total CPU hours for the computed meshes.

3.3 Power Effects

Power effects can be easily included in the model using a box containing the Virtual Blade Model (VBM) mesh or the propeller. These box meshes are coupled with the "main" aircraft mesh by using non-conformal interfaces. This methodology allows rapid changes of propeller modeling and the inclusion of the propeller in frozen rotor or unsteady computations. The "Prop" box is shown in Fig. 4.

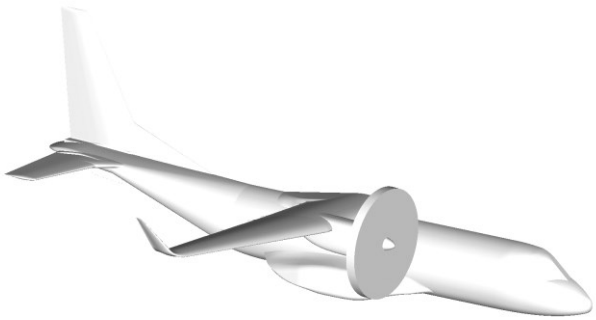

Fig. 4. Propeller box.

3.4 Mesh Smoothing

Due to the poor quality of some cells of the SHM meshes (negative volumes, left handed faces, low thickness boundary layer cells, etc) additional smoothing is required before the mesh can be successfully used for computations. The COTS tool "ANSYS FLUENT meshing" has been used to improve mesh quality.

A typical smoothing process with several smoothing iterations (up to 6 with various percentages of "bad" cells selected) is performed in parallel with 8 CPUS and it takes approximately 2.2 hours clock wall time.

During the same "smoothing" process, mesh is reordered and partitioned.

4 Solving

High Performance Computing (HPC) has been used extensively in a cluster running Linux. The COTS tool ANSYS Fluent has been used for the RANS computations using pseudo-time step integration to decrease the computing time to achieve convergence.

4.1 General Settings

Since most of the computed cases are at low speed (always below Mach 0.5), a pressure coupled solver with segregated energy and turbulence equations is used. A 2 equation turbulence model is selected; a standard k-w Shear Stress Transport (SST) model is used (see [3]). Second order upwind schemes are used for all variables.

4.2 Solution

Solution is advanced in time with a pseudo-time stepping method with explicit relaxation instead of a more classical CFL approach.

The flow is initialized from the free stream condition and latter a Full Multi Grid (FMG) cycle with a density based explicit solver with 5 multi-grid levels is performed with a low CFL. This yields a good starting point for the solution.

A pseudo time-step stair increase is used during the first 200 iterations until the end time value is reached, this time value is kept constant during the rest of the computation.

Computations are performed in approximately 1,900 CPU hours for an average of 4,200 iterations. With the typical 128 CPUs computation, this yield a wall clock time of around 15 hr. Meshes scale well (tested up to

256 CPUs and as low as 96) and wall time can easily be reduced with more CPUs.

4.3 Power Effects

Typical flight computations are performed without power effects, and thus, without the propeller box and wake to reduce cell count and yield results faster. A new mesh is created when propeller effects need to be studied. A compiled VBM UDF is used with data of sections of the propeller at different Reynolds and Mach numbers as well as information of blade twist, RPMs and pitch. Propeller effects are shown in Fig. 5 for a half aircraft on ground.

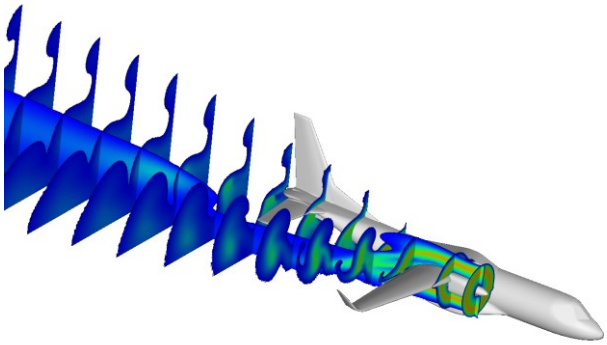

Fig. 5. Ground VBM computation.

4.4 Validation

The flow solution of the new "fast" approach is compared with a traditional structured multi-block approach with y+ 1 boundary layers and a different solver (ANSYS CFX) for a C295W. Results for CL, CD and pitching moment are shown in Fig. 6.

The new methodology shows an average of 4.02% discrepancy in CL (higher than expected), 1.04% in CD (lower than expected) and a large variation of 7.7% in $Cm_{\propto}$. It is thought that this discrepancy in lift and pitching moment is due to the wing wake impinging on the Horizontal Tail Plane (HTP) located in a low position.

Despite this pitching moment issue, the comparison was deemed successful for the purpose of the new methodology as a fast indication of the aerodynamic behaviour and work continued with the new configurations.

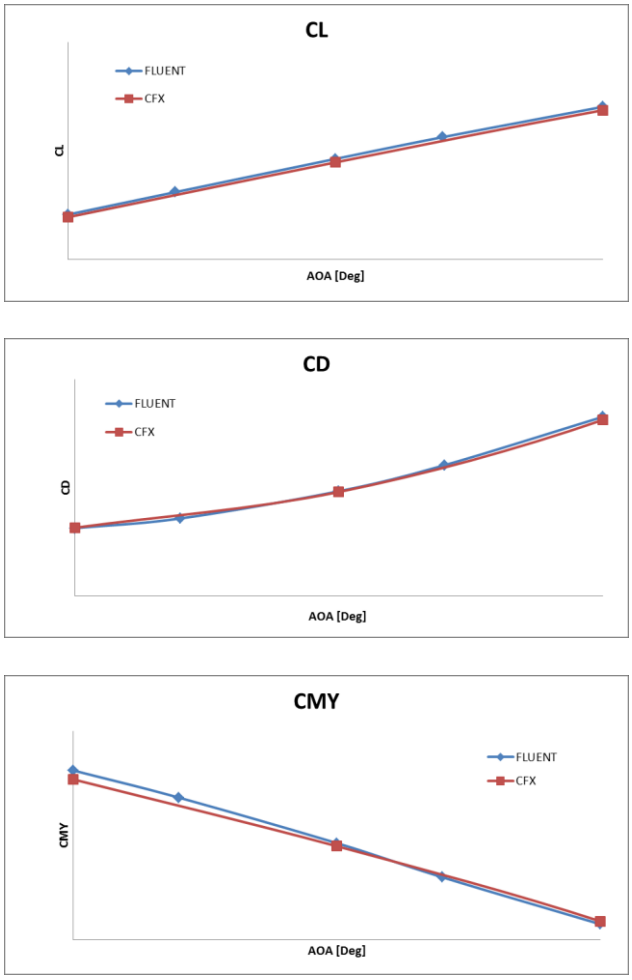

Fig. 6. Force & moment comparison.

4.5 Mesh Sensitivity

Several meshes changing the level 0 size have been performed and analyzed for different aircraft configurations. The mesh level 0 size was changed from the baseline to larger initial mesh sizes. Overall mesh sizes decrease accordingly from 50.6M to 28.6M and finally 18.2M cells. Forces and moments are compared in the following figure (Fig. 7).

Discrepancies in CL averaged 0.9%, CD only 0.8% and again, large variations in the pitching moment, indicating the importance of the wake leading to the HTP resolution for this aircraft.

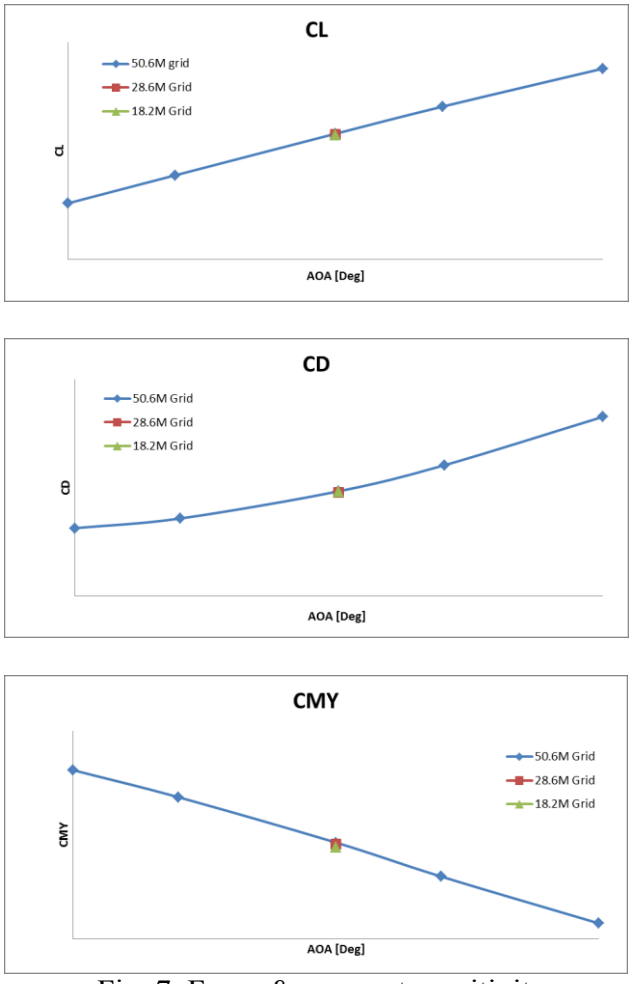

Fig. 7. Force & moment sensitivity.

4.6 Wake Issues

Since the use of a brute force wake creates lots of unnecessary cells, wake adaptive refinement was tested for several aircraft configurations. The use of conservative variable gradients was deemed necessary but some means of protecting the boundary layer regions seem mandatory. Following the idea of blending functions used in some turbulence models (see [6]), several blending function based on wall distance has been tested for robustness and speed. Finally, the following criterion, similar in formulation to a hyperbolic tangent, to protect the boundary layer is used:

$$Crit = 0.5\left(1 + \frac{10 \cdot dist_{wall}^{3} - 1}{10 \cdot dist_{wall}^{3} + 1}\right) \qquad (1)$$

The captured wake with this criterion is shown in Fig. 8, representing the fluid areas with a total pressure decrease non-dimentionalised with dynamic pressure and a threshold of 1.5%.

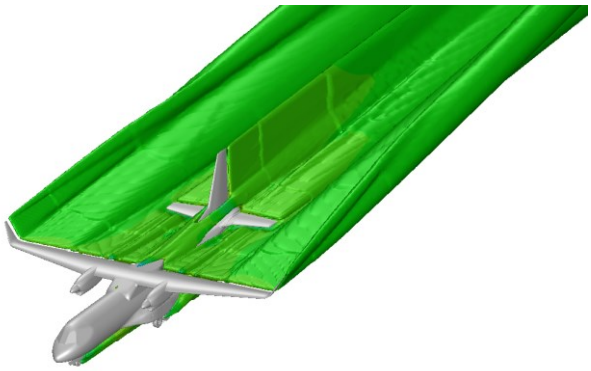

Fig. 8. Wake criteria.

Three grid refinement cycles has been performed using the current criteria starting from the 18.2M grid. Better overall results, especially in the pitching moment, have been obtained. At the end, the computation time using this approach has been similar to the "brute force" wake approach but with higher complexity.

4.7 Run Time

During solution run-time, especially during the initial iterations or right after a time-step change or gradient change, solution might show some "instabilities" and conservative variables might reach unphysical results. A User Defined Function (UDF) implemented in C++ has been added to the solver to cope with such issues.

The CFD solver default trimming between a minimum and maximum value of the conservative variables has been modified. Now, pressure and temperature are not only trimmed but averaged with the remaining partition cells and coordinates of the "departing" cells are provided for mesh enhancement in the region or boundary condition checking.

5 Post-Processing

The flow fields have been post-processed with Ensight 9.x (see [5]). Scripting has been used extensively to compare changes in the flow field due to topology or configuration changes. An example of a C295W with deployed landing gear and open doors is shown in Fig. 9.

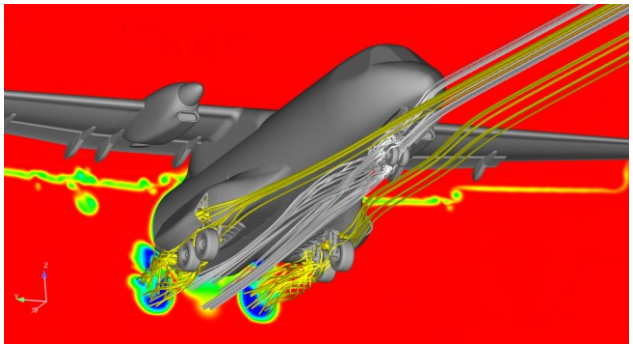

Fig. 9. Total pressure loss.

A detail of the flow in the vicinity of the new landing gear doors is observed in Fig. 10.

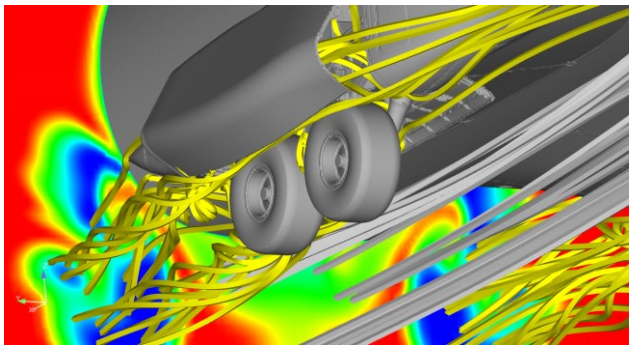

Fig. 10. Total pressure loss near field.

Solution y+ values are within the expected values for its use with boundary layer wall functions, as shown in Fig. 11.

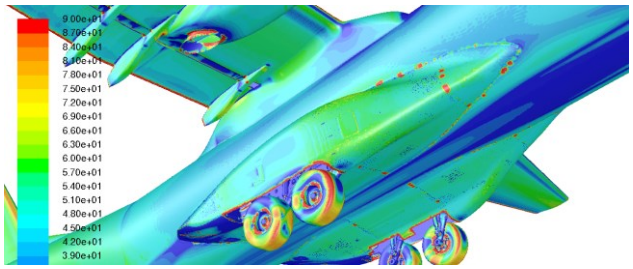

Fig. 11. Y+ values.

Additional effort was put in the SHM mesher settings in an attempt to improve mesh quality and boundary layer resolution in particular.

5.1 Data Averaging

Since pseudo-time stepping is used in the computations, fluctuations in the flow field due to separations are non-negligible. Averaging of all the forces and moments is required. Typically, an average of at least 10% of the solver iterations is performed and statistical values obtained. Lift, drag and pitching moment history results are shown (Fig. 12) corresponding to a C295W at take-off configuration at a typical angle of attack.

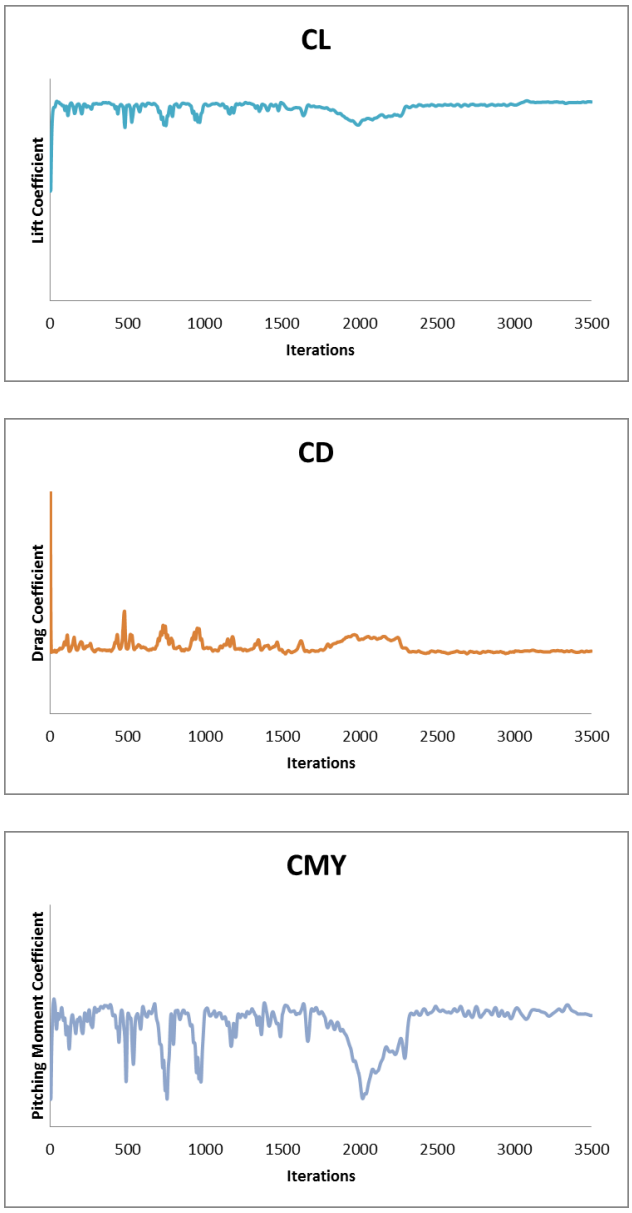

Fig. 12. Run-time forces & moments.

Fluctuations due to change in gradient and slope limiter are clearly visible in the forces and moment shown in Fig. 12 (only 3,500 iterations in this case while typically 5,000 iterations are performed and around 7,500 for the higher angles of attack).

Force and moment data is extracted over all the surfaces of the model in order to integrate

components individually or in groups over any number of iterations (typically 500).

In order to provide pressure loads to the structures department, averaging of the pressure flow field is also performed.

6 Wind-Tunnel Comparisons

During the design process of the new sponson and landing gear a wind tunnel tests campaign has been performed.

Fig. 13 shows the installed wind-tunnel model in the test section with the C295W with new sponson and main landing gear doors.

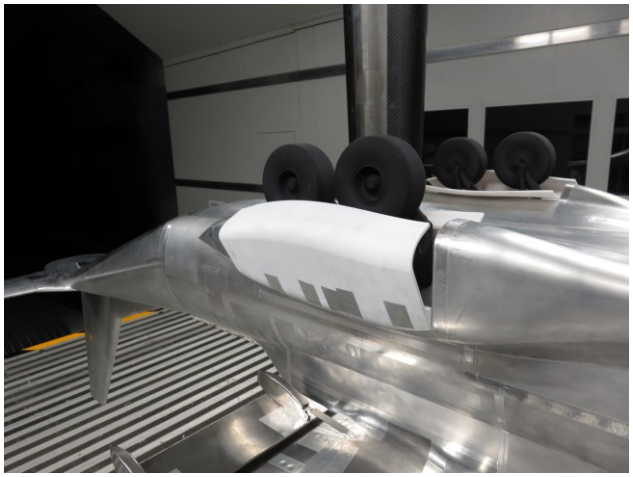

Fig. 13. Wind tunnel test model.

6.1 CFD Modeling

In order to compare CFD results with wind tunnel data, instead of changing model size and creating new meshes due to different BL sizing, static pressure of the far field was changed to match the Reynolds number. This approach reuses current meshes and only changes in boundary conditions are required. The same solver settings have been used with success for these computations.

6.2 CFD vs Wind Tunnel Data

Data from wind tunnel test is compared with a quadratic fit of the computed CFD angles of attack.

Drag increment results for the new sponson and landing gear doors opened with gear down are shown in Fig. 14 with a good general agreement between the CFD and tunnel data. However, the evolution of the drag increment with the lift coefficient on such a configuration has the opposite trend. This can be explained due to the use of wall functions without low Reynolds number corrections at the wind tunnel conditions with the "flight" mesh with its correspondent boundary layer height. Despite the opposite trend, the average drag increment is considered acceptable.

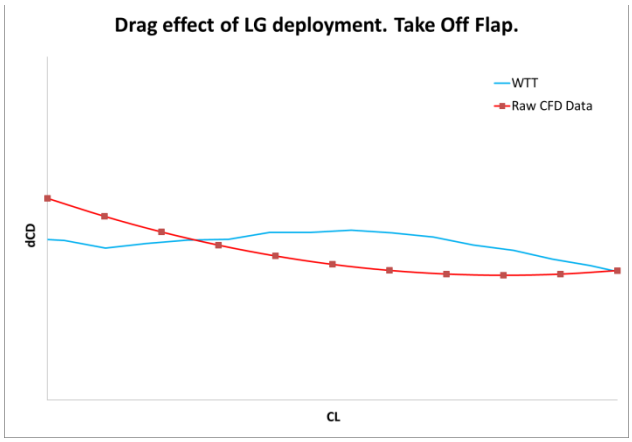

Fig. 14. New landing gear down drag increase.

7 Flight Test Comparisons

In the last quarter of 2017 the new sponson and landing gear doors were first flown in the C295W.

7.1 Aircraft Trimming

In order to compare flight data with CFD data, the forces and moments should be trimmed for the given flight condition. From the lift, drag and pitching moment, the angle of attack and elevator deflection required are computed to obtain null pitching moment for a certain weight and CG position while keeping a constant lift coefficient. Corrections due to altitude, DISA, climb rate or sideslip due to One Engine Inoperative (OEI) conditions are included as well.

7.2 CFD vs Flight Test Data

Data from flight test has been collected and compared with CFD data "trimmed" for the test altitude, CG and weight.

As it can be seen in Fig. 15, CFD data under predicts drag due to the sponson and main

landing gear door changes. However, the trend with angle of attack is good. Drag increments due to flight test boom and trailing cone have been subtracted from the flight test data.

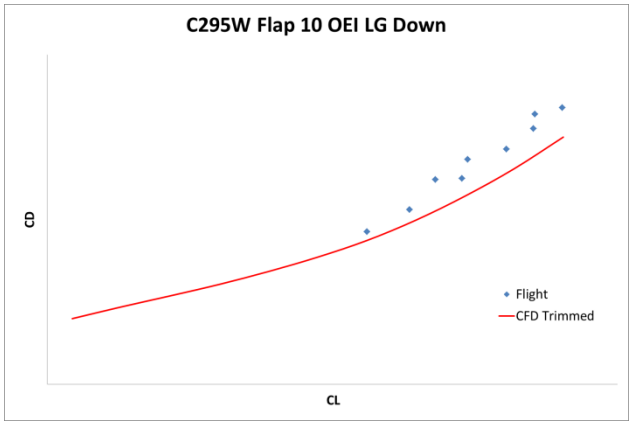

Fig. 15. Flight test comparison.

8 Conclusions

A new "Fast" CFD methodology is introduced reducing the cost of traditional methods while yielding good results for highly complex configurations.

Although more computationally intensive, the overall design cycle time is greatly reduced with the use of automated mesh generation directly from CAD files and CFD parallel computing while reducing the overall engineering time.

CFD results are compared with wind tunnel and flight test data for a landing gear down configuration with acceptable results for the purpose of a fast methodology.

9 Contact Author Email Address

For further comments or questions, please mailto: Carlos.Z.Gonzalez@airbus.com

References

[1] OpenCFD Ltd (ESI Group). *OpenFOAM User Manual Release 2.3*. 2014.

[2] OpenCFD Ltd (ESI Group). *OpenFOAM User Manual Release 3.0+*. 2015.

[3] ANSYS Inc**.** *ANSYS Fluent Theory Guide Release 15.0*. 2013.

[4] ANSYS Inc**.** *ANSYS Fluent UDF Manual Release 15.0*. 2013.

[5] Computational Engineering International, Inc. *EnSight User Manual for Version 9.2*. 2009.

[6] F. R. Menter. *Two-Equation Eddy-Viscosity Turbulence Models for Engineering Applications*. AIAA Journal, 32(8):1598-1605, August 1994.

[7] T. J. Barth and D. Jespersen. *The design and application of upwind schemes on unstructured meshes.* Technical Report AIAA-89-0366, AIAA 27th Aerospace Sciences Meeting, Reno, Nevada, 1989

Copyright Statement